Advance Alerts from Gravitational Wave Searches of Binary Compact Objects for Electromagnetic Follow-ups

A Thesis

submitted to

Indian Institute of Science Education and Research Pune

in partial fulfillment of the requirements for the

BS-MS Dual Degree Programme

by

Shomik Adhicary

Indian Institute of Science Education and Research Pune

Dr. Homi Bhabha Road,

Pashan, Pune 411008, INDIA.

April, 2020

Supervisor: Prof. Sukanta Bose

Certificate

This is to certify that this dissertation entitled Advance Alerts from Gravitational Wave Searches of Binary Compact Objects for Electromagnetic Follow-ups towards the partial fulfilment of the BS-MS dual degree programme at the Indian Institute of Science Education and Research, Pune represents study/work carried out by Shomik Adhicary at Indian Institute of Science Education and Research under the supervision of Prof. Sukanta Bose, Senior Professor, Gravitational Wave Group at the Inter-University Centre for Astronomy and Astrophysics (IUCAA) during the academic year 2019-2020.

Prof. Sukanta Bose

Shomik Adhicary

Committee:

Prof. Sukanta Bose

Prof. Suneeta Vardarajan

This thesis is dedicated to my family and friends who believed in me even when I did not believe in myself

Declaration

I hereby declare that the matter embodied in the report entitled Advance Alerts from Gravitational Wave Searches of Binary Compact Objects for Electromagnetic Follow-ups are the results of the work carried out by me at the Gravitational Wave Group at the Inter-University Centre for Astronomy and Astrophysics (IUCAA) and at the Indian Institute of Science Education and Research, Pune, under the supervision of Prof. Sukanta Bose and the same has not been submitted elsewhere for any other degree.

Shomik Adhicary

Prof. Sukanta Bose

Acknowledgments

I thank Prof. Sukanta Bose for his patience and expert guidance. I was an amateur in this field. I had a lot to learn and a lot of knowledge to amass. He helped me at each and every step of my journey. For this, I extend my deep and sincere gratitude to him.

I thank Prof. Suneeta Vardarajan for being the Expert in my Master's Thesis. This project would not have been possible without her unwavering support, help and advice.

I thank Sunil Choudhary and Sudhagar Suryaprakasam for helping me get familiar with all the software and taking time to make sure I understand the intricacies of my project. Their helpful advice was key in progressing my work in this project.

I thank Anwesha Maharana, Niramay Gogate, Prasanna Joshi, Prasham Jain, Rahul Poddar and Raj Patil for all their support and discussions I had with them. This really helped me overcome the obstacles in my work and shaped my thinking.

I thank Aarcha Thadi, Akshay Nair and Sanjana Manjunath who were always there to uplift my spirits, provide tough love and help me get across the finish line.

I also thank the Indian Institute of Science Education and Research (IISER), Pune and Department of Science and Technology's (DST) Innovation in Science Pursuit for Inspired Research (INSPIRE) Scholarship for Higher Education (SHE) for giving me the opportunity to be a part of their programme. This would not have had such an enriching experience without their support.

I also thank the Inter-University Centre for Astronomy and Astrophysics (IUCAA) for their hospitality, services and accepting me as a project student. I acknowledge the use of IUCAA Laser Interferometer Gravitational-Wave Observatory (LIGO) Data Grid (LDG) cluster Sarathi for the computational/numerical work.

Contents

Abstract

The first binary neutron star inspiral was observed on 17^{th} Aug 2017 at 12:41:04 UTC by Advanced LIGO and Advanced Virgo. The signal, GW170817 had multiple electromagnetic counterparts – a γ-ray burst and other transients. We expect more mergers of this kind to occur in subsequent years. These systems emit gravitational waves while falling into one another. With the help of a network of gravitational wave detectors, one can localize the source in the sky using the gravitational wave signal before the merger. The localization information can be passed on to telescopes in order to observe the system in the electromagnetic regime. In this way, maximum possible information about the binary can be extracted. This method is known as Advance Alert. In this thesis, we demonstrated that Advance Alert can be made faster and more efficient using Particle Swarm Optimization. We show that this method is faster than the current Advance Alert implementation in the detection aspect. With a faster detection, we will have more time to locate the source and observe it. If this method is optimized, it will provide us with a viable technique to observe such systems and aid in multi-messenger astronomy.

List of Figures

List of Tables

Conventions

This chapter clarifies all basic concepts / terms / definitions which are repeatedly used in this thesis.

Fourier transform $\tilde{u}(f)$ in frequency domain of a time domain signal $u(t)$ is defined as

$$\tilde{u}(f) = \int_{-\infty}^{\infty} u(t) e^{-2\pi i f t} dt$$

and the inverse Fourier transform is defined as

$$u(t) = \int_{-\infty}^{\infty} \tilde{u}(f) e^{2\pi i f t} df$$

Complex conjugate of a value x is denoted as x^*

Matched filter is defined as

$$\langle a|b\rangle(t) = 4Re \int_0^{\infty} df e^{2\pi i f t} \frac{\tilde{a}(f)\tilde{b}^*(f)}{S_n(|f|)} \tag{1}$$

where

a, b: Time domain Signals

S_n: Power Spectral Density

Masses are reported in units of solar mass

$$1M_{\odot} = 1.989 \times 10^{30} kg$$

Chapter 1

Introduction

This introductory chapter will give an overview of gravitational waves (GWs), detectors used to search for GWs, search methods employed for detecting GW signals from astrophysical sources and electromagnetic counterparts associated with GW events. It will go over the motivation and basics of the primary problem this thesis tries to address – Advance Alert. Chapter 2 examines how various programs and algorithms related to advance alert were implemented. Chapter 3 steps through the results obtained from this work. Chapter 4 discusses the achievements and shortcomings of the approach followed in this thesis which combines the developments of chapters 2 and 3 and reviews its validation through the results obtained. Chapter 5 summarizes the final important results of this thesis work and implications for future research.

1.1 Gravitational Waves

Einstein's Theory of General Relativity (GR) can be summarized by Wheeler's famous quote: [29]

Matter tells space how to curve. Space tells matter how to move.

General relativity is a generalization of special relativity and Newton's law of gravity. It gives a unified description of gravity as a geometric property of spacetime. The curvature of spacetime is directly related to whatever energy and matter are present around it. The relation is specified by a system of partial differential equations known as the Einstein field equations.

Gravitational waves are linear perturbations to an otherwise flat spacetime. Therefore, we can write the metric $g_{\mu\nu}$ as a sum of the flat Minkowski metric $\eta_{\mu\nu}$ and a small perturbation $h_{\mu\nu}$:

$$g_{\mu\nu} = \eta_{\mu\nu} + h_{\mu\nu}$$

The linearized vacuum Einstein equation in Lorentz gauge for a small perturbation is [36]

$$(-\frac{\partial^2}{\partial t^2} + \nabla^2)\bar{h}^{\mu\nu} = 0$$

where $h_{\mu\nu}$ is a tensor in 'background' Minkowski spacetime.

We can see that this is a wave equation. It is known as the 3D Wave Equation. Solutions to these equations in the Lorentz, transverse-traceless gauge predict gravitational waves [21].

$h_{\mu\nu}$ can be estimated in a similar way that electromagnetic waves are calculated from Maxwell's equations. Hence, gravitational waves have similar properties as that of electromagnetic waves. They travel at the speed of light. In GR, gravitational waves are produced by the quadrupole moment and higher moments. Due to conservation of mass, momentum and angular momentum, the radiation from the mass monopole, mass dipole and momentum dipole disappear, respectively.

Energy carried away by gravitational waves follows a $1/r^2$ law. This implies a $1/r$ fall-off in the gravitational wave strain. They also interact very weakly with matter making them hard to detect.

Gravitational waves are transverse and have two independent polarizations. The polarizations

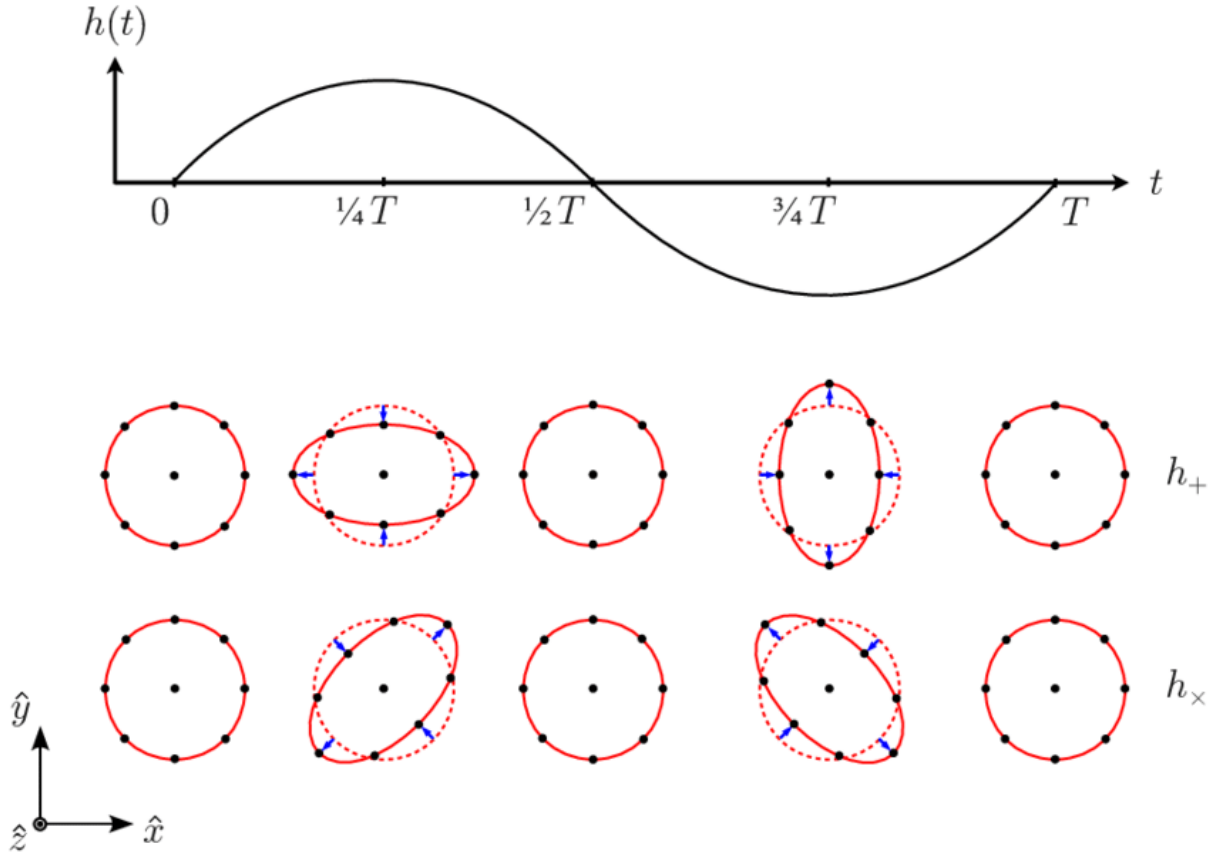

Figure 1.1: A monochromatic gravitational wave of period T propagating along Z-axis [25]

are off from each other by $\pi/4$ radians. Hence, the 2 independent polarizations can be thought of as 'plus' $(+)$ and 'cross' $(\times)$. When a monochromatic, linearly polarized gravitational wave is passing perpendicularly through a ring of particles, particles in one directions are stretched away from each other in a sinusoidal fashion. Particles in the perpendicular direction to this axis are stretched closer to one another. In the 2nd half of the cycle, the stretching is reversed. This is shown in Fig.1.1.

The stretching and squeezing caused by the gravitational wave results in a change in distance (δL) between two freely falling objects. The strain is defined as the instantaneous difference between the fractional length change $(\delta L_1 - \delta L_2)$ between two perpendicular directions. We expect gravitational wave strain on Earth to be the order of 10^{-21} [12].

1.2 Detectors

In 1959, Weber had designed a bar detector in order to detect gravitational waves [44]. Later in 1975, Hulse and Taylor discovered a binary pulsar of two neutron stars [23]. As gravitational waves carry energy and momentum away from the system, their orbit shrinks. They calculated the shrink and it agreed well with the estimation from GR [45]. Although indirect, this was the first evidence for gravitational waves.

The current detectors in use are known as Advanced Laser Interferometer Gravitational-Wave Observatories (aLIGO) [1], Virgo [7] and GEO600 [8]. There are two aLIGO detectors located at Hanford and Livingston, United States of America. The Virgo detector is located at Cascina, Italy; While GEO600 is located at Sarstedt, Germnay. These detectors are essentially Michelson interferometers as seen in Fig.1.2.

Each arm of an aLIGO detector is around 4km in length. Assuming the strain of an incoming gravitational wave to be 10^{-21}, it will result in a differential length change of 4×10^{-18}m. For comparison, the average radius of a nucleus of an atom is around 10^{-15}m.

This sensitivity is achieved by adding modifications to the simple Michelson interferometer. One of the modifications done to the Michelson interferometer is adding a Power Recycling Mirror between the Laser and the Beam-Splitter. It allows photons to pass through it from the laser to the beam-splitter. When the light comes back from the interferometer, it reflects it back into the interferometer. In this way, the power in the detector is recycled which facilitates a buildup of power in the interferometer. This buildup coupled with the resonant arms cavities amplifies the sensitivity. On top of this, the whole optical set-up is seismically isolated with the help of multiple pendulum systems. This prevents vibrations of the earth caused by tectonic motion, vehicles travelling, tree cutting and other factors that affect the motion of the mirrors (Test Masses). A vacuum is maintained in the tubes and kept at low temperatures to minimize thermal fluctuations. This minimizes the effect of stray atoms interfering with the light's path. A Signal Recycling Mirror (SRM) is also placed in between the interferometer and the Photodiode. The SRM is used to 'tune' the

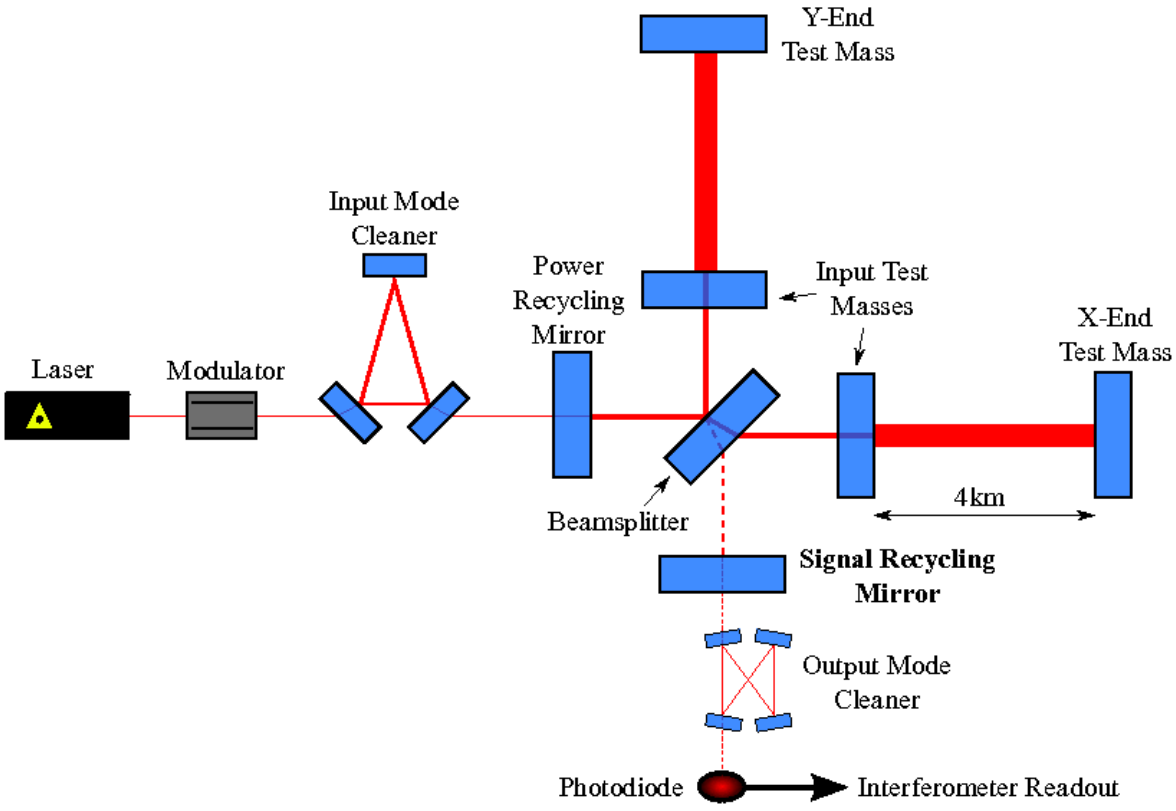

Figure 1.2: aLIGO Schematic
[18]

detector's response in a certain frequency band. This is similar to tuning a radio receiver to listen a specific station at a given frequency. An amalgamtion of all these factors result in an increased sensitivity of the interferometer to measure the extremely small differential length changes. The output is measured at the photodetector and converted to strain. These detectors are sensitive in the frequency range of 10 Hz to a few kHz. Their targets include GWs from the coalescence of compact binary objects and continuous waves from neutron stars [19].

Future detectors similar to aLIGO have been commissioned. Detectors like Kamioka Gravitational Wave Detector (KAGRA), LIGO-India, Einstein Telescope (ET) and Cosmic Explorer will be part of this network in the coming future. To observe gravitational waves in the frequency range lower than aLIGO, a space-based interferometer – Laser Interferometer Space Antenna (LISA) has been commissioned. Apart from interferometers, Pulsar Timing Array (PTA) can also be used to detect gravitational waves. They are sensitive in the frequency range of 10^{-9} to 10^{-7} Hz. Their primary aim is to constrain the stochastic gravitational wave background.

1.3 Gravitational Wave Searches

The first direct detection of a gravitational wave was from the coalescence of two black holes. It was detected on 14^{th} September 2015 by aLIGO detectors [5].

The detectors are used to search for gravitational waves from a variety of sources. The sources can be classified into 3 classes: -

1. Bursts
    - Chirp signals from Compact Coalescing Binaries
    - Non-axis-symmetric Supernovae
2. Stochastic Background

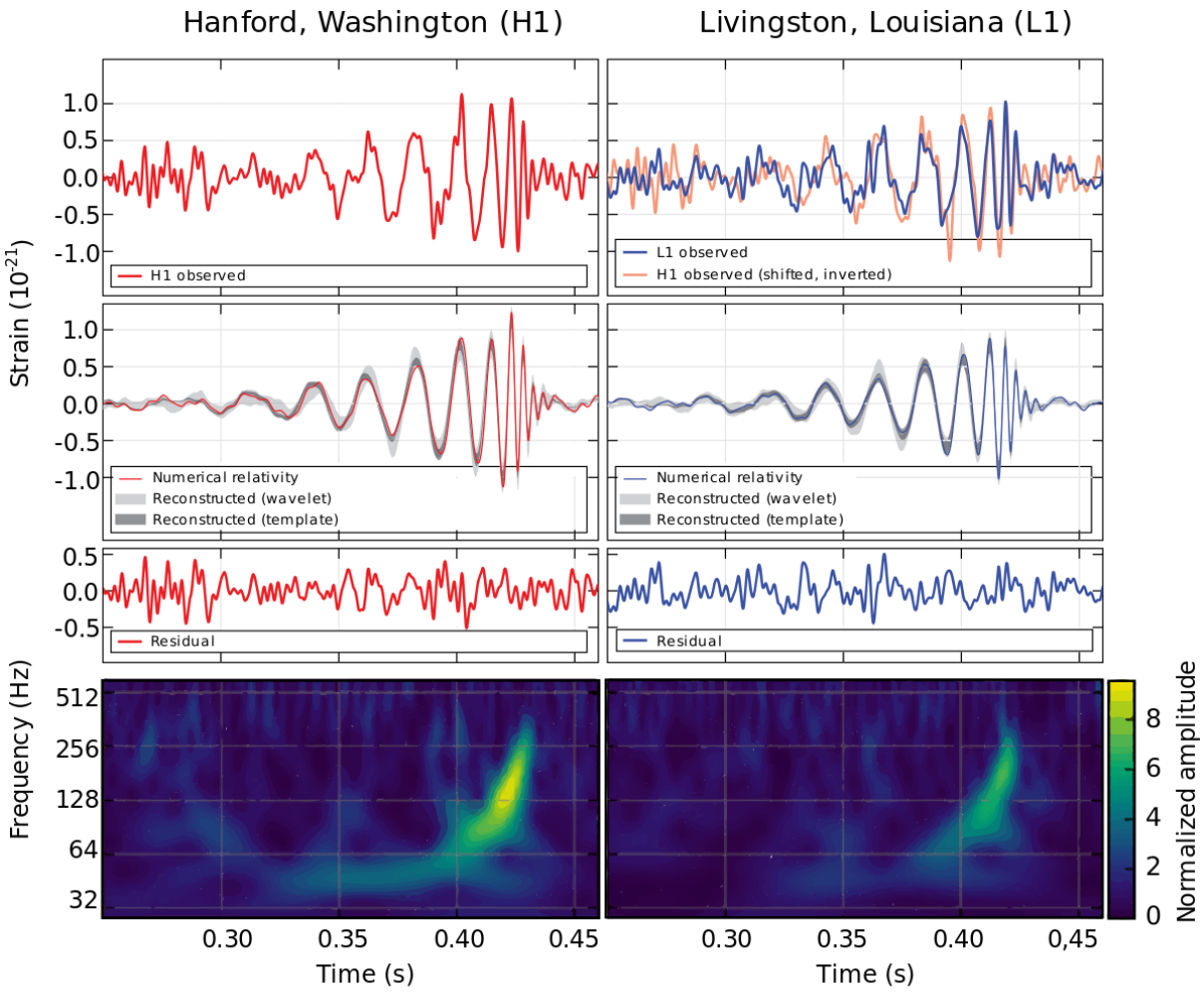

Figure 1.3: GW150914
[5]

3. Continuous Emitters

    - Non-axis-symmetric Neutron Stars

Burst sources produce transient signals which can be observed for a short period of time and can be searched for using matched-filtering techniques. Stochastic background is a long lived process and can be estimated using cross-correlation methods. Continuous emitters are also fairly long lived, but have low amplitude. Specialized methods which account for the modulation of the signal are used to search for them [11].

This thesis' primary focus is on detecting chirp signals from binary compact objects, especially when at least one object in the system is a neutron star. These types of signals consists of 3 parts: -

1. Inspiral: Part of the signal where the objects are still distinct and emitting low amplitude GWs detectable by aLIGO detectors
2. Merger: Part of the signal where the objects are close to another and emitting high amplitude GWs detectable by aLIGO detectors
3. Ringdown: Part of the signal where the objects have merged into one object and emitting very low GWs detetctable by aLIGO detectors

1.4 Electromagnetic Counterparts

If at least one object in the system is a neutron star (NS), it is expected that the merger would be visible in the electromagnetic (EM) domain – short Gamma Ray Bursts (GRBs), broadband afterglow and kilonovae [27]. To gain information from this system, the telescopes must be looking at the system during the merger.

Being able to observe a compact binary coalescence in both EM and gravitational wave (GW) regime will provide us with a host of information. It gives information of an event in two different

regimes. This is the basis of multi-messenger astronomy. With this combined knowledge, we can put constraints on the NS-Equation of State (EOS), understand nature of short GRBs, r-process nucleosynthesis, jet formation, calculate the difference between speed of light and gravitational waves, and other tests of GR [17].

We expect there to be a few coincident GW and EM observations every year [28]. There are plans underway to search for EM counterparts of GW signals in different parts of the EM spectrum like gamma-ray, X-ray, optical and radio [2], [22], [4].

1.5 Advance Alert

The technique of Advance Alert involves detecting and locating a Compact Binary Coalescence (CBC) before its merger and relaying that information to telescopes in order to detect it in the EM regime. This allows us to view the event in different regimes and obtain a plethora of information. For a binary neutron star system, the GW signal could be observed for 10-20 minutes in the aLIGO detectors [35]. Part of the incoming signal, while still in the inspiral phase can be used to approximately detect and locate such a source. We can break up the Advance Alert problem into 2 smaller problems: -

1. Detection of Inspiral part of a Binary Neutron Star (BNS) system in noisy aLIGO data
2. Localization of the BNS system on the 3D sky for EM observations

The algorithm has to work with a truncated signal as estimates are made before the merger. Hence, the Signal to Noise Ratio (SNR) will be lower than that of the full signal. Hence, number of false triggers (background rate) will be high. The background rate increases exponentially as the SNR decreases [12]. The area of localization is also broad $\sim$100-1000 deg^2 [30].

Amplitude and frequency of the GW signal increases with time. Therefore, collecting more of

the signal, results in a higher SNR and a better localization. Evolution of the localized area with time and SNR can help in the advance alert problem. With more detectors on the way, the area should shrink to $\sim$ 10-100 deg^2 [6].

As the event is ephemeral, algorithms need to be fast in predicting the sky position.

1.6 Gravitational Waves Data Pipeline

In this thesis, the focus will be on the data collected by the LIGO-Virgo Collaboration (LVC) which is analyzed to search for gravitational wave signals from Compact Binary Coalescence (CBC) [15]. The Gravitational Waves Data Pipeline for coalescing binaries is a series of operations. It takes raw data as input and outputs a list of candidate events.

Only the data in stable operation mode is used in the pipeline. To get the detector in stable operation mode, it must be locked. Light inside the detector must be made resonant by aligning the optical components such that the light at the anti-symmetric port is a bit off from the minimum. Once the detector is locked, the operator and a LIGO member on duty known as scimon decide whether the data is suitable to be classified as Science Mode. Only Science Mode data can be used for processing. There are multiple ways in which the lock can be lost. The detector must be brought back into stable operation mode before acquiring proper science mode data [12].

The GW signal coming from a binary neutron star system can be modelled well by numerical relativity and other phenomenological techniques [24]. Theoretical waveforms of chirp signals have been accurately calculated [11]. In this thesis, we are concerned only with the inspiral part of the signal since we have to detect and localize the source before merger. This is well modelled by the post-Newtonian approximation. An example of the signal is shown in Fig.1.4. The merger happens at 0s. Here, the signal still has 40s left until merger. The blue part of the signal has not reached the detector yet.

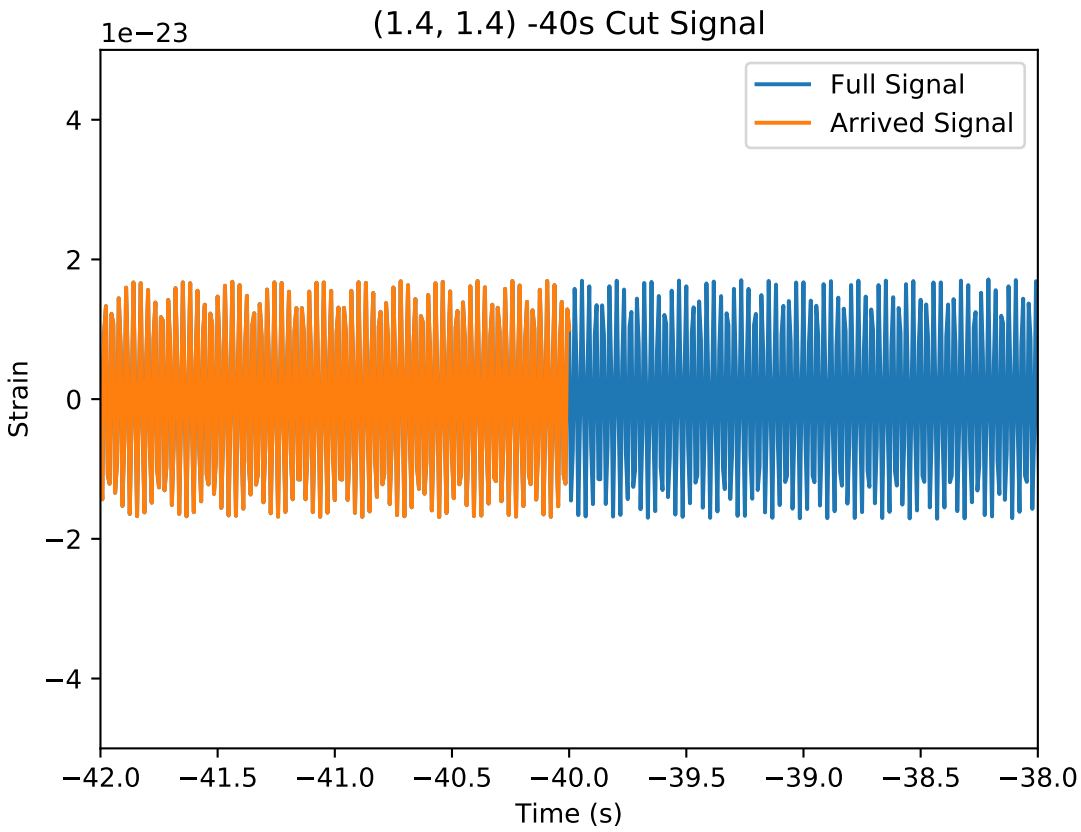

Figure 1.4: Partial GW signal from a BNS merger compared to entire signal

1.6.1 Template Banks

The chirp signal from CBC depends on multiple parameters as mass, spin, sky position and others [39]. In the second observation run 2 (O2) of LVC, the masses and aligned spins of the system were considered while searching for CBCs [14]. No knowledge of the incoming signal is known a priori. Hence, a template bank of expected signals is required to search for the signal in the data [33].

A template bank is a set of waveforms which are generated from the parameters of the system within a certain range using the Power Spectral Density (PSD) of a data chunk. Each point in the parameter space gives a different waveform. The placement of these points is determined by the mismatch (M) between the waveforms. Mismatch is defined as the fractional loss of Signal-to-Noise Ratio (SNR) when the signal does not exactly match with the template.

$$M = 1 - \frac{\langle h|s\rangle}{\sqrt{(\langle h|h\rangle \langle s|s\rangle)}}$$

where

M: Mismatch

h, s: Time-domain Templates

If we assume that CBCs are distributed uniformly in the parameter space, then we lose M^3 of the population. The number of templates decreases if we accept more mismatch (less stringent condition) between the templates. The number of templates also depends on the shape of the PSD of the detector. The PSD changes over time. Hence, a new bank must be generated for every new data segment. LALSuite [16], LALInference [42], PyCBC [31] and GstLAL [26] are currently used for generating template banks. Maximum mismatch of 3% is chosen between neighbouring templates as standard.

The number of templates in a template bank increases exponentially as the number of parameters increase. This is because additional sub-spaces are added to the parameter space as the number

of independent parameters are increased. The time required to search for a signal in data is linearly proportional to the number of templates.

The primary problem of advance alert as explained in Section 1.5 is early detection and not parameter estimation. Hence, only the component masses of the system are used to generate this template bank. The waveforms generated are the simplest, but the most efficient [35]. The primary aim of this thesis is to detect a BNS system before merger. The choice of mass range for this is 1 $M_\odot$ to 3 $M_\odot$.

aLIGO is sensitive from 10 Hz in the frequency domain. This puts a lower cutoff on from where we can start looking for the signal. During a real-time search, the incoming frequency of the GW signal is unknown. Hence, multiple template banks with different cut-off times have to be generated for advance alert. Each template bank consists of templates that end at a certain time before the merger. Each template bank has a gap of 5s from the other. A search is done for templates from 80-40s before merger.

Most BNS GW signals will reach $\sim$ 30 Hz by $\sim$ 60 s before merger. A template bank with starting frequency as 10 Hz and cut-off frequency as 30 Hz between the 1 $M_\odot$ to 3 $M_\odot$ range with maximum mismatch of 3% is shown in Fig. 1.5. There are $\sim$ 7000 templates in this bank represented by individual dots. The colour code is used to show the chirp mass of each pair.

Chirp Mass is defined as

$$\mathscr{M} = \frac{(m_1 m_2)^{3/5}}{(m_1 + m_2)^{1/5}}$$

where

$\mathscr{M}$: Chirp Mass

m_1, m_2: Component Masses

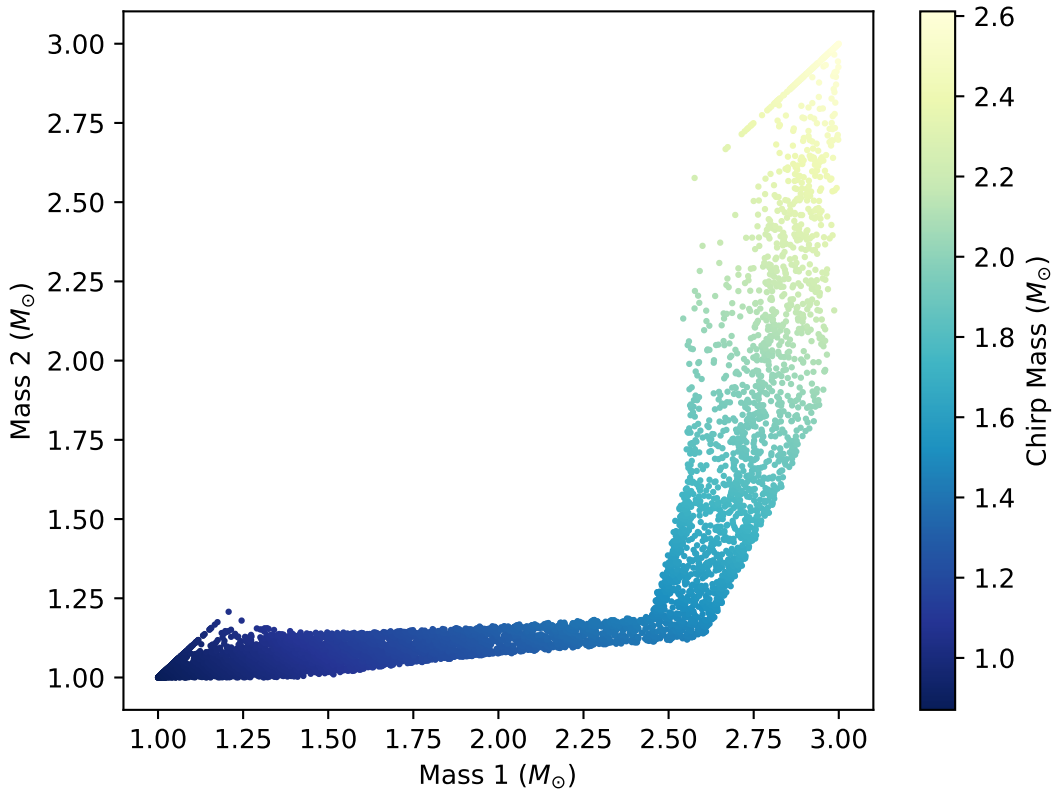

Figure 1.5: Template Bank Example with starting frequency 10 Hz and cut-off frequency as 30 Hz between the 1 $M_\odot$ to 3 $M_\odot$ range with maximum mismatch of 3%. Colour code shows the chirp mass of the system.

1.6.2 Detection

The template bank provides a set of possible waveforms that could exist in the data. Matched filtering techniques are used to search for these signals in LIGO data. Consider a data stream $d(t)$ which is a sum of signal $s(t)$ and noise $n(t)$

$$d(t) = s(t) + n(t)$$

Assume that $n(t)$ is stationary noise i.e. a random noise whose probability of lying within any given interval does not change with time. A matched filtering operation to find the correlation between the template $h(t)$ and data $s(t)$ must be done in order to find a signal within the data. It is the most important test in the search for GW events in LIGO data [3]. The SNR for a template $h(t)$ obtained after matched filtering is [10]

$$\rho^2(t) = \frac{1}{\langle h|h\rangle} |\langle s|h\rangle(t)|^2$$

where $\langle a|b\rangle$ is defined in Eq. 1 of Conventions.

In reality, the noise in the detector is non-stationary and non-gaussian. The non-gaussian transients that occur in the detector are known as 'glitches'. The glitches may have high power and can pass the matched filter test. This will increase the background rate [41]. In order to remove the glitches and test the consistency of the signal with the template, we employ the χ^2 test. There are several χ^2 based tests that are used to veto different types of glitches. In this thesis, the most common one – the traditional χ^2 test has been used.

The χ^2 test works by taking the data in frequency domain and dividing it into a fixed number of bins of equal power. For every bin, consistency of the signal is checked with respect to a template. A reduced χ^2 test is used in the pipeline. A value close to 1 implies that the signal is consistent with the wave form. The reduced χ^2 test is given by

$$\chi_r^2 = \frac{p}{2(p-1)} \frac{1}{\langle h|h\rangle} \sum_{j=1}^{p} |\langle s|h_j\rangle - \frac{\langle s|h\rangle}{p}|^2$$

where

p: Number of Frequency Bins

h_j: Part of template h in j^{th} bin

Once detected using a particular detector using matched filtering [34] and a χ^2 test [9], coincidence in time of the signal in other detectors, consistency of the parameters and the amplitudes [13] are checked to classify it as a true signal. Finally, a Bayesian inference test – likelihood ratio is calculated. Likelihood ratio is defined as the ratio of probability of Signal being Present to that of Signal being Absent. The log-likelihood measure when h is the time-domain template and s is the time-domain data comes out to be [32]

$$ln(\lambda) = \langle s|h\rangle - \frac{1}{2}\langle h|h\rangle$$

1.6.3 Localization

After detection, that segment of data along with parameters of the trigger are inputted to BAYESTAR [38]. BAYESTAR is a Bayesian and Markov Chain Monte Carlo (MCMC) algorithm that can localize the source within 15-20s. Information about the localization should be sent to the telescopes about 20s before the merger. This will give them enough time to orient themselves optimally. Hence, the signal must be detected at least 40s before merger [35].

Merger of a BNS system is ephemeral in time. In order for advance alert to succeed, the source must be detected and localized as fast as possible. The primary factors to take into account are the area of localization and response of telescopes. Response of telescopes is defined as the time taken by telescopes to cover a given area in the sky. It depends on how the localization area changes with time and SNR. Knowing this information will help devise a strategy to search the localized area.

1.7 Particle Swarm Optimization

Particle Swarm Optimization (PSO) [20] was originally developed in order study the sociological behaviour of animals living together in colonies; For instance, swarms. It is a stochastic algorithm that eventually converges to the optimal solution (maximum or minimum) of a given function in the parameter space. PSO is a random global optimization algorithm.

The individuals in the swarm are social. Hence, they can communicate with one another. This enables every individual to access all the information gathered by swarm. PSO can be implemented by initializing certain number of particles randomly in the parameters space with some random velocity. Each particle's trajectory is determined by three independent traits: –

1. Inertia: The tendency to move in the same direction. If a particle is moving in a certain direction it will continue to move in that direction
2. Nostalgia: The tendency to move towards its Personal Best (pBest). Each particle has a tendency to move towards the best location found by it
3. Knowledge: The tendency to move towards the Global Best (gBest). Each particle has a tendency to move to the best location found by the swarm

The velocity of a particle is a sum of these three traits

$$v_{i,d}(t+1) = \omega v_{i,d}(t) + \gamma_p r_p[p_{i,d}(t) - x_{i,d}(t)] + \gamma_g r_g[g_d - x_{i,d}(t)]$$

where

v: Velocity

i: Individual Agent

d: Dimension

t: Time

ω, γ: Strengths

r: Stochastic Factors (Randomized at each iteration)

p: Personal Best (pBest)

g: Global Best (gBest)

x: Current Position

The three independent traits are weighted differently. These are determined by the 'strengths'. At every iteration, the tendency of each particle to move towards pBest or gBest is determined randomly. The force of attraction towards pBest and gBest is assumed to follow a harmonic potential. The algorithm is evaluated in time steps of 1 unit. Hence, the position evolution equation is simply given by

$$x_{i,d}(t+1) = x_{i,d}(t) + v_{i,d}(t)$$

In this thesis, the template bank approach was replaced by a PSO based approach. It is used to maximize the likelihood function and find optimal solutions in the parameter space.

1.7.1 PSO Variants

Different extensions like multiple swarms, relay searches and, independent or hostile swarms can be incorporated into the algorithm. The algorithm outputs the gBest after a set number of iterations. There are various boundary conditions that can be implemented.

Multiple Swarms

The parameter space is searched by multiple swarms instead of one. This can be accomplished in two ways

1. Independent: Each swarm evolves independently. They can be evolved simultaneously because of this. This approach can be parallelized.

2. Relay: Swarms evolve subsequently. Information gathered by past swarms is passed on to consecutive swarms. It can be used give priors on solutions and restrict the parameter space.

1.7.2 Advantages

PSO is non-discreet as it can access the entire parameter space. It is computationally inexpensive comapared to TB since it does not have to generate TBs and instead generates templates dynamically. It learns during the search by using information gathered by all agents and samples points accordingly. The increase in computational time with increase in parameters does not scale as much as it does with TBs. It is faster, more effective, recovers more signals and has better parameter estimation accuracy [39]. Hence, these properties of PSO can be used to make searches better overall. It was proposed by Wang and Mohanty for implementation in Gravitational Waves (GW) analysis [43].

Chapter 2

Methods

All analysis was done on IUCAA LDG Cluster Sarathi. The computer nodes with 40 cores was primarily used for the work. All values and times quoted are run-times on these nodes. PyCBC [40] functions were used in this thesis.

2.1 Template Bank

pycbc_geom_nonspinbank was used to generate the template bank. Only the inspiral part of the waveform is relevant and time is of the essence. Hence, simplest the possible waveforms without spin are considered. The default value of 70 Hz for the dynamic scaling factor is used. This is relevant for calculating metrics and re-scaling. aLIGO is sensitive from 10 Hz. Hence, the lower frequency cutoff is kept at 10 Hz. Most BNS system waveforms reach 30 Hz 60s before merger. Hence, the upper frequency cutoff is kept at 30 Hz. Waveforms of interest can be observed in the aLIGO detector for $\sim$100s. Hence, the corresponding delta-f value is (1/100s) 0.01 Hz. The minimum match between two neighbouring templates is kept as the default value of 0.97. The mass range is kept as 1.0 $M_{\odot}$ to 3.0 $M_{\odot}$ as it is expected to find BNS systems within this range. The ethnica metric was not calculated in order to save time in template bank generation. The

aLIGOZeroDetHighPower PSD was used to generate the PSD for the template bank. The options used to generate this template bank are summarized in Table 2.1.

Option	Description	Value
pn-order	Post Newtonian Order to be used	zeroPN
f0	Dynamic Scaling Factor	70 Hz
f-low	Lower Frequency Cutoff	10 Hz
f-upper	Upper Frequency Cutoff	30 Hz
delta-f	Frequency Spacing	0.01 Hz
min-match	Minimum Match	0.97
min-mass1	Minimum Mass of First Object	1.0
min-mass2	Minimum Mass of Second Object	1.0
max-mass1	Maximum Mass of First Object	3.0
max-mass2	Maximum Mass of Second Object	3.0
psd-model	Analytical Model of the PSD	aLIGOZeroDetHighPower

Table 2.1: Options with their corresponding description and values for generating the template bank

2.2 Matched-Filtering Operation

Matched-Filtering Operation (MFO) takes the most amount of time. It can be considering as the rate determining step. An MFO consists of several steps.

2.2.1 Template Generation

The first step involved in an MFO is Template Generation. *pycbc.waveform.get_td_waveform* was used to generate templates in time domain. The approximant used was SpinTaylorT4. Only the inspiral part is relevant. Only component masses were used to generate the template. The sampling rate for full signals was 2048 Hz and that of cut signals was 128 Hz. The delta_t was determined by the sampling rate $dt = \frac{1}{\text{Sampling Rate}}$. Full templates started from 30 Hz, while cut templates started from 10 Hz. The template and the data chunk are made the same length.

2.2.2 Power Spectral Density Generation

The PSD is generated next. It has half the length (accounting for 0 and length being an integer value) of the time domain resized template. *pycbc.psd.aLIGOZeroDetHighPower* was used to generate the PSD. The delta-f corresponded to the resized template's delta_f.

2.2.3 Matched Filtering

The next step involves calculating the SNR. The SNR for each template was calculated by *pycbc.filter.matched_filter*. It takes the template, data chunk, PSD and lower frequency cutoff as input. The maxima of the absolute value of SNR was reported to be the SNR of a given template.

2.2.4 Updating

At each step, the newly calculated SNR is compared with the maximum SNR obtained. If the new SNR is greater, the maximum SNR is accordingly changed and the parameters of the corresponding template are held in memory.

2.2.5 χ^2 Test

Only if the Updating is necessary, the χ^2 test is performed. This is done to reduce computation time as the χ^2 test requires Fourier Transforms (FTs) and division of power in equal bins which are computationally expensive. *pycbc.vetoes.power_chisq* is used to calculate the power χ^2 value. It takes template, data chunk, PSD and lower frequency cutoff as input. The result is normalized by the degrees of freedom

$$\text{Degrees of Freedom} = 2 \times \text{Number of Bins} - 2$$

The power χ^2 value corresponding to the maximum absolute SNR value is reported as the template's power χ^2.

2.3 Particle Swarm Optimization

This section briefly goes over steps involved in the implementation of the PSO algorithm.

2.3.1 Initialization

The particles in PSO need a parameter space to search for the signal. This parameter space is the same as that used in the template bank approach . It has two dimensions – the component masses of the binaries. The range of the parameter space is from 1.0 $M_\odot$ to 3.0 $M_\odot$. This is chosen as our target source is BNS systems. It is expected that BNS systems lie within this range [35].

A swarm of 200 particles is initialized. This includes initializing their position and velocity. The first component mass is chosen from a uniform distribution of the mass range. The second component mass is chosen from a uniform distribution between the lower limit of the mass range (1.0 $M_\odot$) and the first component mass. The waveform generated by component masses (m_1, m_2) will be the same as the waveform generated by component masses (m_2, m_1). Hence, the choice of the second component mass is done such to avoid redundancies while searching through possible waveforms.

Each particle is assigned a random velocity. The maximum possible absolute velocity is $1/10^{\text{th}}$ of the mass range. This is done so that each particle moves at an optimal pace to cover the parameter space. Velocity in each direction is chosen from a uniform distribution between the positive and negative value of the maximum possible absolute velocity. The initial pBest of each particle is the position of the particle itself. The gBest of the swarm is not assigned in the initialization process. It is evaluated after the first iteration of the PSO algorithm.

2.3.2 Evolution

The evolution of the swarm is dictated by the equations in Section 1.7. It is done in discrete time steps of 1 unit. After every step, the previous gBest is compared with the current gBest and it is updated accordingly. The position with the higher SNR is considered better.

2.3.3 Boundary Condition

The Reflecting Boundary Condition was used in this implementation. This was chosen to ensure particles stay close to the boundary if the best possible match is close to the boundary as well. When a particles crosses a boundary, its position is mirrored onto the boundary and its velocity is reflected. It is also ensured that the particles stay only on side of the parameter space ($mass_1 \geq mass_2$) by a similar boundary condition. This is to ensure there is no redundancy while going over templates as explained in 2.3.1.

2.3.4 Termination

The termination of the algorithm is done by a stop condition. In this case, maximum number of steps is used. The algorithm is run for 18 steps. This ensures that (18×200) 3600 Matched Filtering Operations (MFOs) are done in the entire run. The template bank approach has $\sim$ 7000 MFOs. The choice of 18 steps is to have around half the number of MFOs in the template bank approach and enough time for the algorithm to detect a signal. The value of gBest along with the SNR and χ^2 is outputted. This is considered to be the optimal value.

2.4 Cut Templates

The inspiral part of the signal is the main focus of the thesis. The detection must also happen 40s before merger. In order to simulate such signals, the signals were randomly cut in the time-domain between 80s - 40s before merger. The problems associated with this are discussed in Section 3.4. In order to fix this problem, an one-sided tukey window was applied to the template after the cut. Another approach was to zero pad the template on both sides before taking the FT which was also problematic.

The approach which was finally used was to generate the templates in the frequency-domain itself and process the data in the frequency-domain as well. The (1.4, 1.4)$M_{\odot}$ template was taken as the proxy for all templates. The instantaneous frequency of this template at various cutoff times was used as the upper frequency cutoff while generating templates. The (1.4, 1.4)$M_{\odot}$ template was converted to its analytical form using *scipy.signal.hilbert*. The instantaneous phase of the signal was calculated by using *numpy.angle*. Differentiation of the instantaneous phase divided by the sampling rate in radians gives the instantaneous frequency.

2.5 Parallelization

Python *multiprocessing* module was used to achieve parallelization in the implementation. The MFO is the slowest step. MFOs are also independent of each other. Hence, this step was chosen to be parallized first to get maximum benefit in reduction of computation time. Each template has a different length. Hence, each template's MFO takes different amount of times to run. Equally dividing all the templates between the cores would not be fruitful. Hence, Python's *multiprocessing.Pool.apply_async* was chosen as the cores could be utilized to their maximum potential. Once a core finishes performing a template's MFO, it can start processing the next template's MFO.

2.6 Pipeline

The PSO algorithm for cut templates can be incorporated in two ways.

1. Relay: Each swarm is run consecutively. The -80s swarm will be run first. It will be followed by the -75s swarm, -70s swarm and so on. The gBest, pBest and final positions of the particles is passed on from swarm to the next. This is continued until the -40s swarm outputs its gBest.

   It is expected that the particles find the early part of the signal with the initial swarms. This will help subsequent searches to focus only on a certain region of the parameter space. Thereby, the particles will converge faster as they do not have to search for the best possible position. It also eliminates time required to initialize.

2. Independent: All swarms are run independently on different machines. They pass on their output to one single separate machine and start processing the next data chunk. The separate machine plots and checks whether the SNR is progressively increasing with time. It checks whether the χ^2 value is below threshold for each swarm. It also checks the average gBest position of each swarm and their spread.

   All swarms are running simultaneously and independently which serves as a good check and reduces time required to run the algorithm. If the data contains a signal, the SNR must increase with time as more of the template will match with the data. It is expected that this implementation can observe this phenomena. The χ^2 checks are to ensure glitches do not pass through. The average and spread of gBest values are checked to ensure that all swarms have come to a similar conclusion.

Chapter 3

Results

3.1 Template Bank

The template bank which was generated is shown in Fig. 1.5. There are ∼7000 templates. Each point on the graph represents a template that goes through MFOs for each data chunk. It takes 6 mins on average for the template bank search to run.

3.2 Matched-Filtering Operation

Each MFO takes 2s on average to complete. The data that is inputted consists of a signal randomly injected in a stream of randomly generated aLIGO noise. Fig. 3.1a shows an example of such data. The blue part of the graph represent what the detector observes. The orange part of the data is the signal buried in the noise. After an MFO, the SNR and χ^2 time series is outputted. The corresponding SNR and χ^2 time series for the signal in Fig. 3.1a is shown in Fig. 3.1b. The blue part of the graph represents the absolute SNR as a time series. The maximum absolute SNR comes out to be 8.85. The orange part of the graph represents the χ^2 value as a time series. The

corresponding χ^2 value to the maximum absolute SNR is 1.59 in this case. The χ^2 peaks before and after the maximum SNR value. This is better shown in Fig. 3.2. The colour scheme in this figure is the same as that followed in Fig. 3.1b. The values correspond to a different injection. This graph shows how the χ^2 value peaks just before and after the maximum absolute SNR value.

3.3 Particle Swarm Optimization

The PSO implementation can discriminate between BNS system signals and glitches on the same level as template bank search. This is evidenced by Fig. 3.3. This graph shows the χ^2 vs. the SNR for 100 glitches and 100 signals in aLIGO noise after going through a PSO search. The signals are represented in blue, while the glitches are represented in orange. The signals must have high SNR to be detected and low χ^2 to be consistent with the template. Glitches will have high SNR and pass the SNR test, but will also have high χ^2 values which will be indicative that they do not match the template. As seen in Fig. 3.3, we can see that the glitches and signals are well separated. Any trigger with SNR > 8 (threshold for aLIGO is 8) and $\chi^2 < 3$ (threshold for aLIGO is 4) can be classified as a signal.

The PSO based approach takes 220s on average to run. This is faster than the current template bank based approach.

3.4 Cut Templates

The time-domain cut template matched exactly with the time-domain full template. This can be seen in Fig. 3.4. The FT of a cut template matched well with the full signal, albeit around the cut – there were oscillations around the cut frequency. This was expected as a Discrete FT (DFT) was performed on the template. This effect is shown in Fig. 3.5. As mentioned in Section 2.4, an one sided tukey window was applied after the cut in the time-domain. This helped reduce the

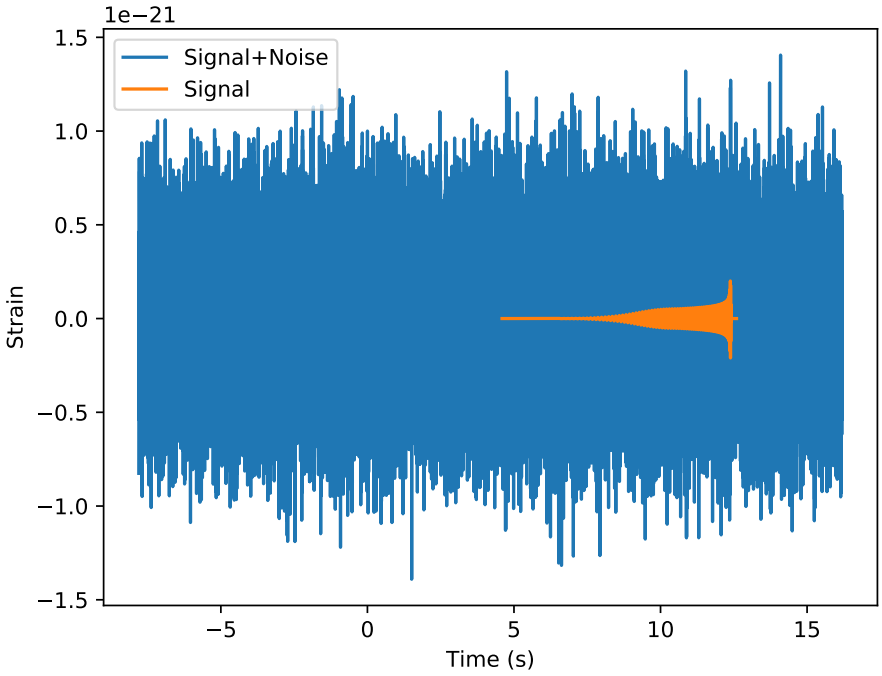

(a) Signal Randomly Inputted in a Stream of Randomly Generated aLIGO Noise (Input)

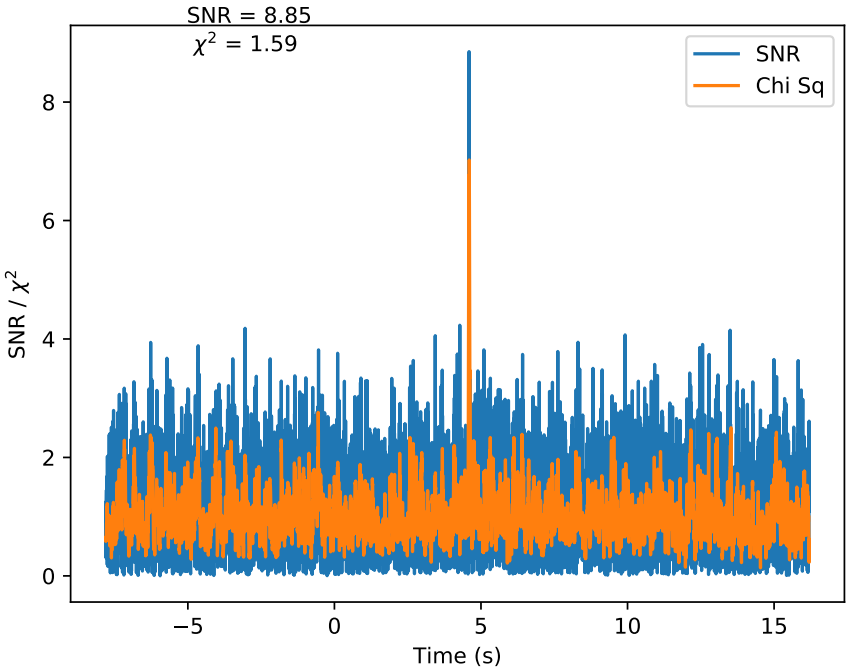

(b) SNR and χ^2 Time Series of the Signal

Figure 3.1: Example of Data Inputted and Outputted for an MFO (Output)

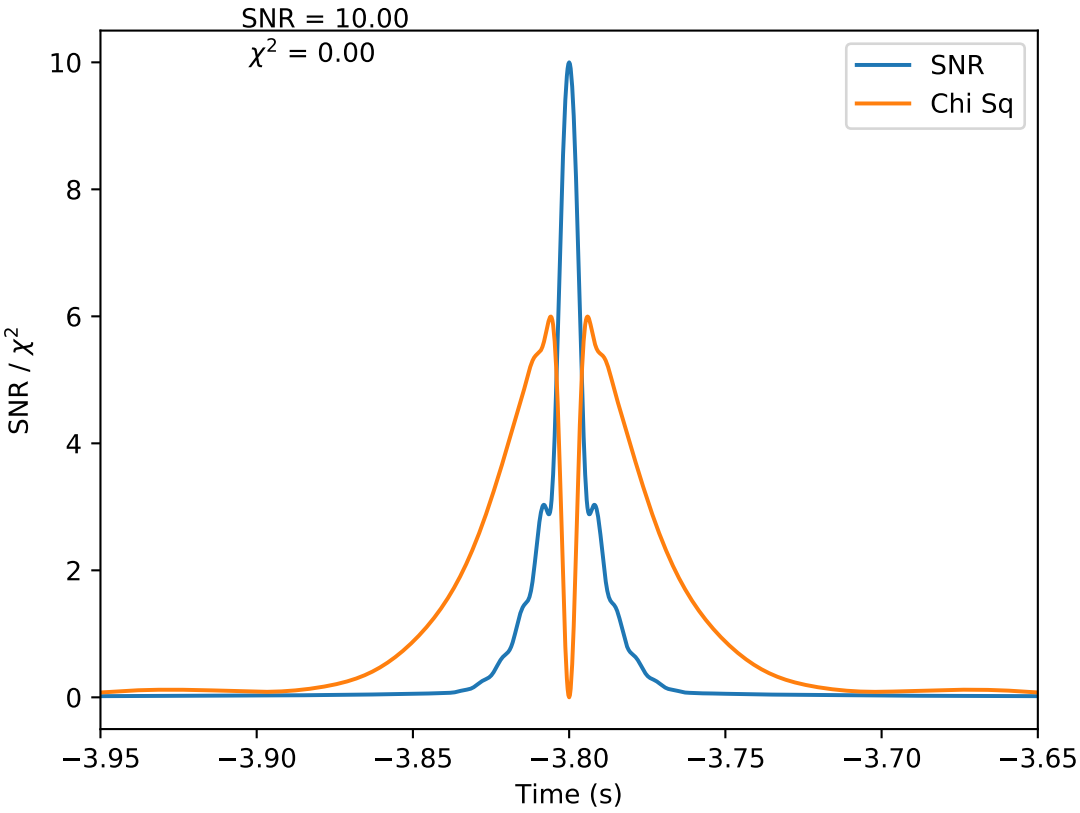

Figure 3.2: SNR and χ^2 Time Series of the Signal

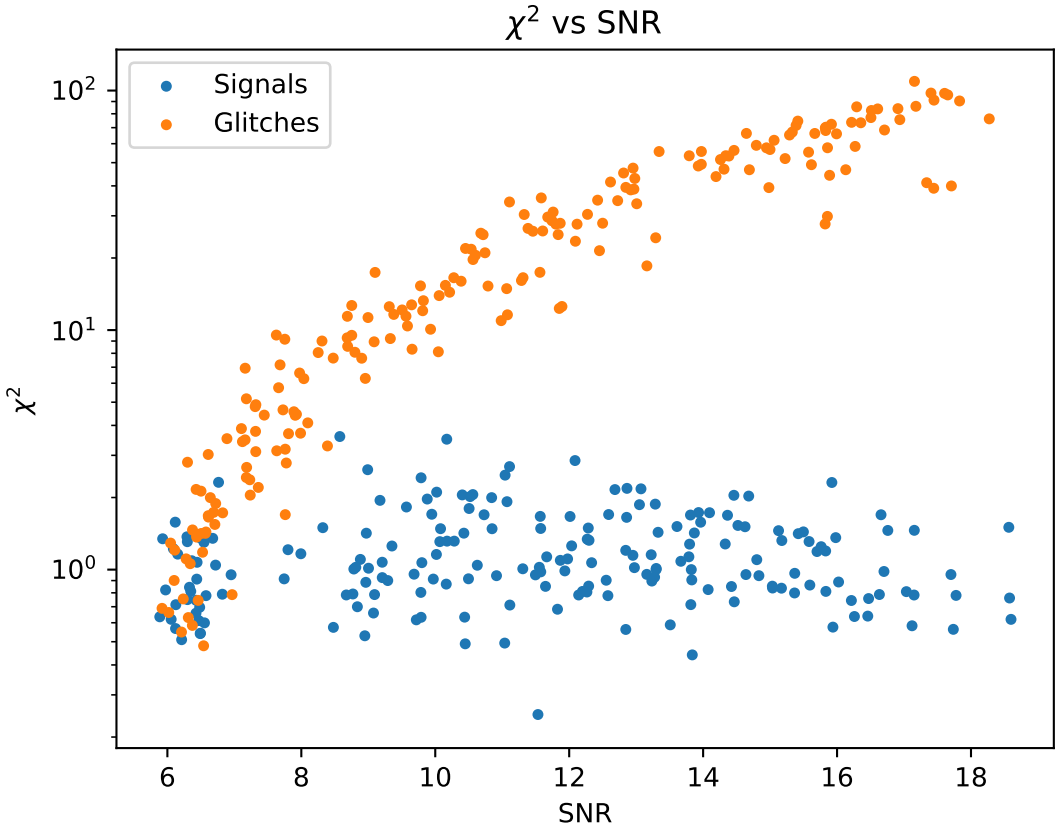

Figure 3.3: χ^2 vs SNR for Glitches and Signals in Noise for PSO

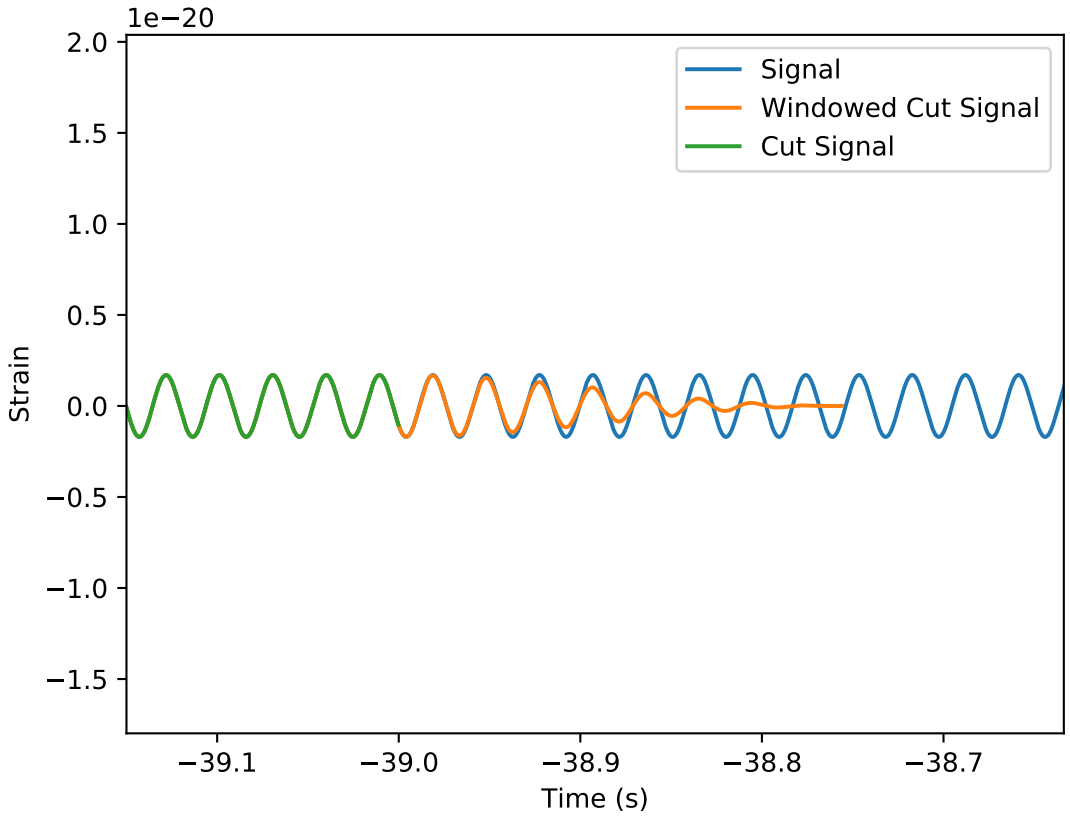

Figure 3.4: Full Signal, Cut Signal at 39s before merger and One-Sided Tukey Windowed Cut Signal in Time-Domain

magnitude of the oscillations as also seen in Fig. 3.5. As the length of the window is increased, the magnitude of the oscillations decreases. This is evidenced in Fig. 3.6. The blue line shows the FT of the cut template, while the orange line shows the FT of a windowed template of a certain window length. The shorter window (window length of 100 points) is quite similar to the cut template and has discernible oscillations. As we increase the window length (up to 900 points), the oscillations die out, but we have more template to process which will increase computation time.

Examples of templates generated in the frequency-domain are shown in Fig. 3.7. There are no oscillations in these templates. They are full signal templates. For different time cut templates, these frequency-domain templates are considered only up to a certain upper frequency cutoff as estimated by the procedure outlined in Section 2.4.

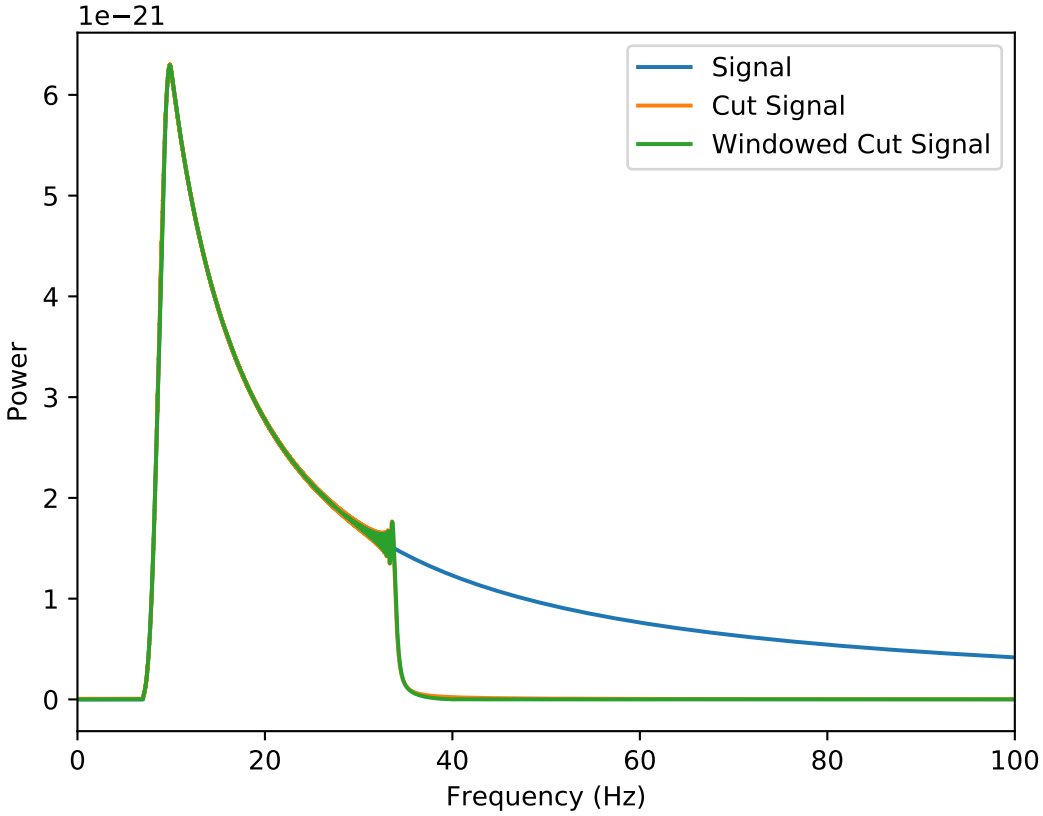

Figure 3.5: Full Signal, Cut Signal at 39s before merger and One-Sided Tukey Windowed Cut Signal in Frequency-Domain

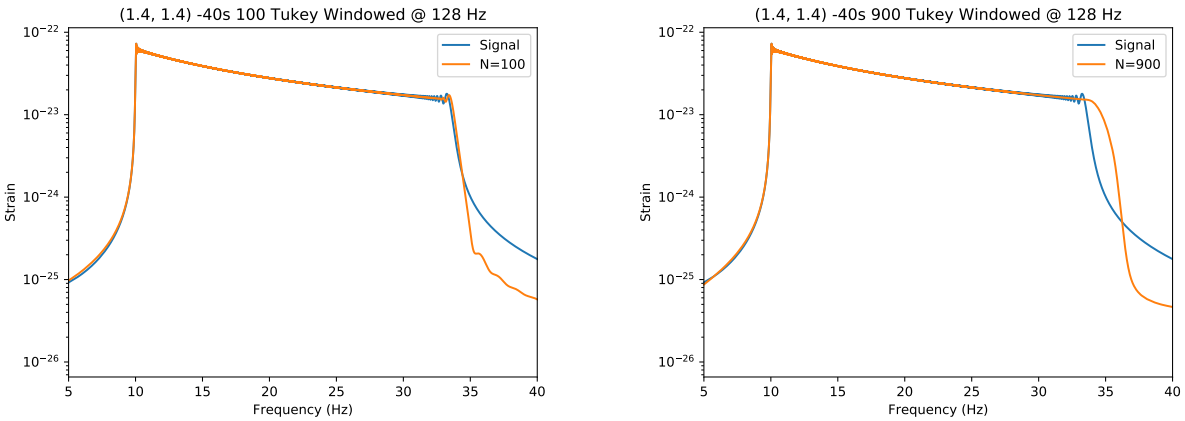

(a) Window Length = 100 Points

(b) Window Length = 900 Points

Figure 3.6: Windowed Templates with Different Lengths of Window

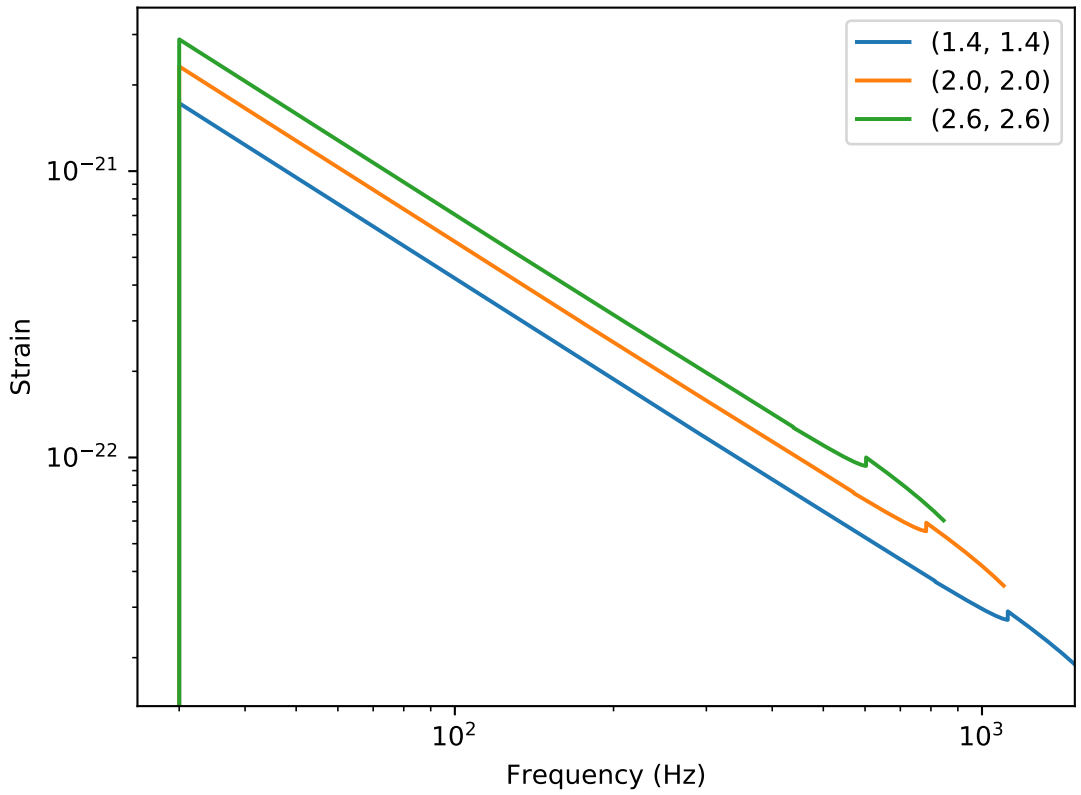

Figure 3.7: Templates Generated in Frequency-Domain of Three Different Instances of BNS systems

3.5 Pipeline

The relay search takes 25 mins on average to run. The problem associated with this implementation was that the bias in results gets propagated through the swarms. For example, if there is a glitch in the data, the particles swarm around the template which matches the glitch well. This causes the subsequent swarms to explore only the region around this template and the bias gets propagated. A possible way to avoid this is discussed in Chapter 4.

The independent search takes 33 mins on average to run. This is due to the fact that the proposed infrastructure has not been properly set up. All swarms were run independently on a single computer node one after another. The results of one of these searches is shown in Fig. 3.8. The blue line represents the SNR of the signal as a function of time and the orange line represents the χ^2 of the signal as a function of time. The time shows how many seconds before merger are remaining (0s is time of merger). The SNR increases as a function of time. The χ^2 remains lower than threshold for the entire duration and starts stabilizing at the end. The information obtained from this graph gives more confidence to the fact that the observation is a signal.

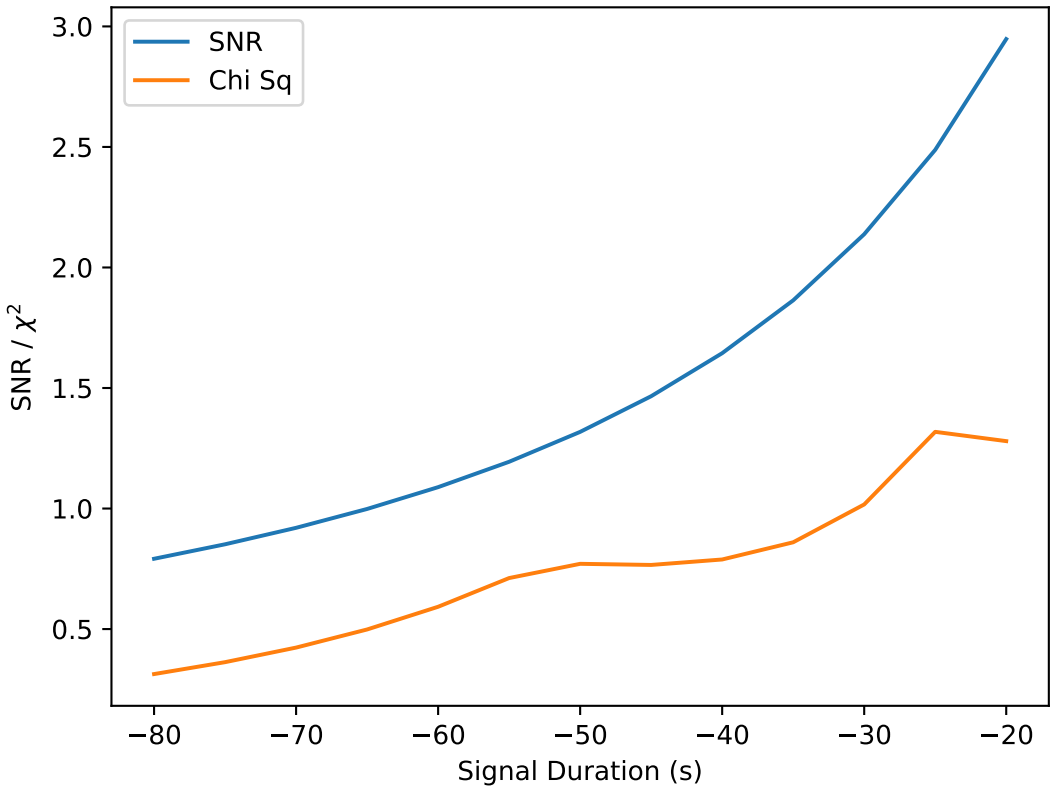

Figure 3.8: SNR and χ^2 of a Signal as a Function of Time Calculated by Independent Search Pipeline

Chapter 4

Discussion

In this thesis, only the mass range of BNS systems was considered. The results for other mass ranges may vary.

The template bank approach to detect GW signals is a tried and tested method. However, it is slow and computationally expensive. A new template bank must be generated for every new data chunk to be analyzed. It requires a check of the entire parameter space which consists of thousands of templates. A computationally expensive MFO must be done for each of these templates.

On the other hand, PSO is a fairly new approach. In this thesis, it has been shown that this method is effective in finding GW signals. It eliminates the need to generate a new template. Instead of exploring the entire parameter space, it learns from the MFOs calculated and samples the parameter space accordingly. These factors make it faster than the template bank approach. This agrees well with previous work done using PSO [39] where they required less number of MFOs to achieve better parameter estimation. It will also aid proposed multi-messenger astronomy searches [35].

The advanced alert problem can be tackled more effectively using the template bank approach due to its speed and efficiency. With the help of parallelization and proper architecture of the data

pipeline, searches in real time can be made possible.

The code used, systems it was run on and the architecture proposed are not optimized to achieve the best possible outcome. There are various shortcomings in the work done which can be fixed and improved upon in the time to come.

If the signal lies in the region of space very close to the boundary, it will be hard for PSO to detect it effectively as the reflective boundary condition does not allow particles to stay in that region.

The relay search method could be improved by reducing the parameter space for subsequent swarms instead of passing on information directly. This would help reduce bias.

Instead of initializing randomly, the agents can be initialized similar to the density of templates in a certain region of the template bank. This might lead to a more efficient search and faster detection.

Another approach that could be tried is to run PSO and perform a template bank search in a certain region around the global best. This could help with better sky localization as with cut signals, parameter estimation is not very good. This information could be passed on to BAYESTAR. This could enable BAYESTAR to work faster.

In PSO, one agent can follow the steepest descent algorithm. This agent could converge on the local maxima quickly while the others could explore the region. When a better maxima is found, this agent could shift to that region and find the local maxima in the new region quickly. Hence, PSO might be able to locate the true global maxima better with this approach.

Subsequent work on this project would be to use PSO itself to localize the source on the sky. This eliminates the need of data transfer to BAYESTAR. It also allows PSO to process more of the signal. This could help to localize the source better. The pipeline could send out an alert and still process the incoming data. At the end of the event, the final localization can be sent to the telescopes for even better viewing.

The final work would involve estimating the distance to the source [37]. This will eliminate certain galaxies in the sky. Thus, reducing the area the telescopes need to search. Hence, the search can be made faster.

Chapter 5

Conclusion

This thesis has compared the traditional template bank approach to the novel PSO based approach. It has looked into some aspects of optimization of both approaches. The PSO based GW signal detection code for partial as well as full GW signals has been successfully implemented. It can differentiate between simulated glitches and signals well.

The major takeaway from this thesis is the fact that the PSO based approach is faster than the template bank based approach and also effective in searching for GW signals from BNS systems. This gives us more time to detect and localize the source better. The method can be improved and optimized, thus making real-time searches a reality and aiding in multi-messenger astronomy. This will enable us to view events similar to GW170817 in both GW and EM domain and extract maximum possible information from the system.

Bibliography

[1] J. AASI, B. ABBOTT, R. ABBOTT, T. ABBOTT, M. ABERNATHY, K. ACKLEY, C. ADAMS, T. ADAMS, P. ADDESSO, R. ADHIKARI, ET AL., *Advanced ligo*, Classical and quantum gravity, 32 (2015), p. 074001.

[2] J. ABADIE, B. ABBOTT, R. ABBOTT, T. ABBOTT, M. ABERNATHY, T. ACCADIA, F. ACERNESE, C. ADAMS, R. ADHIKARI, C. AFFELDT, ET AL., *Implementation and testing of the first prompt search for gravitational wave transients with electromagnetic counterparts*, Astronomy & Astrophysics, 539 (2012), p. A124.

[3] B. P. ABBOTT, R. ABBOTT, T. ABBOTT, M. ABERNATHY, F. ACERNESE, K. ACKLEY, C. ADAMS, T. ADAMS, P. ADDESSO, R. ADHIKARI, ET AL., *Gw150914: First results from the search for binary black hole coalescence with advanced ligo*, Physical Review D, 93 (2016), p. 122003.

[4] ——, *Localization and broadband follow-up of the gravitational-wave transient gw150914*, The Astrophysical journal letters, 826 (2016), p. L13.

[5] B. P. ABBOTT, R. ABBOTT, T. ABBOTT, M. ABERNATHY, F. ACERNESE, K. ACKLEY, C. ADAMS, T. ADAMS, P. ADDESSO, R. ADHIKARI, ET AL., *Observation of gravitational waves from a binary black hole merger*, Physical review letters, 116 (2016), p. 061102.

[6] B. P. ABBOTT, R. ABBOTT, T. ABBOTT, M. ABERNATHY, F. ACERNESE, K. ACKLEY, C. ADAMS, T. ADAMS, P. ADDESSO, R. ADHIKARI, ET AL., *Prospects for observing and*

localizing gravitational-wave transients with advanced ligo, advanced virgo and kagra, Living Reviews in Relativity, 21 (2018), p. 3.

[7] F. ACERNESE, M. AGATHOS, K. AGATSUMA, D. AISA, N. ALLEMANDOU, A. ALLOCCA, J. AMARNI, P. ASTONE, G. BALESTRI, G. BALLARDIN, ET AL., *Advanced virgo: a second-generation interferometric gravitational wave detector*, Classical and Quantum Gravity, 32 (2014), p. 024001.

[8] C. AFFELDT, K. DANZMANN, K. DOOLEY, H. GROTE, M. HEWITSON, S. HILD, J. HOUGH, J. LEONG, H. LÜCK, M. PRIJATELJ, ET AL., *Advanced techniques in geo 600*, Classical and quantum gravity, 31 (2014), p. 224002.

[9] B. ALLEN, *A chi-squared time-frequency discriminator for gravitational wave detection*, 2004.

[10] B. ALLEN, W. G. ANDERSON, P. R. BRADY, D. A. BROWN, AND J. D. E. CREIGHTON, *Findchirp: An algorithm for detection of gravitational waves from inspiraling compact binaries*, Phys. Rev. D, 85 (2012), p. 122006.

[11] P. R. BRADY, T. CREIGHTON, C. CUTLER, AND B. F. SCHUTZ, *Searching for periodic sources with ligo*, Physical Review D, 57 (1998), p. 2101.

[12] D. A. BROWN, *Searching for gravitational radiation from binary black hole machos in the galactic halo*, 2007.

[13] L. CADONATI, *Coherent waveform consistency test for ligo burst candidates*, 2004.

[14] T. D. CANTON AND I. W. HARRY, *Designing a template bank to observe compact binary coalescences in advanced ligo's second observing run*, 2017.

[15] L. S. COLLABORATION, *Analysis of ligo data for gravitational waves from binary neutron stars*, Phys. Rev. D, 69 (2004), p. 122001.

[16] L. S. COLLABORATION, *Ligo algorithm library—lalsuite, free software (gpl), doi: 10.7935*, GT1W-FZ16, (2018).

[17] T. L. S. COLLABORATION AND THE VIRGO COLLABORATION, *Gw170817: Measurements of neutron star radii and equation of state*, 2018.

[18] T. COMMISSARIAT, *Ligo detects first ever gravitational waves – from two merging black holes*, (2011).

[19] J. D. CREIGHTON AND W. G. ANDERSON, *Gravitational-wave physics and astronomy: An introduction to theory, experiment and data analysis*, John Wiley & Sons, 2012.

[20] R. EBERHART AND J. KENNEDY, *Particle swarm optimization*, in Proceedings of the IEEE international conference on neural networks, vol. 4, Citeseer, 1995, pp. 1942–1948.

[21] A. EINSTEIN, *Approximative Integration of the Field Equations of Gravitation*, Sitzungsber. Preuss. Akad. Wiss. Berlin (Math. Phys.), 1916 (1916), pp. 688–696.

[22] P. EVANS, J. FRIDRIKSSON, N. GEHRELS, J. HOMAN, J. OSBORNE, M. SIEGEL, A. BEARDMORE, P. HANDBAUER, J. GELBORD, J. A. KENNEA, ET AL., *Swift follow-up observations of candidate gravitational-wave transient events*, The Astrophysical Journal Supplement Series, 203 (2012), p. 28.

[23] R. A. HULSE AND J. H. TAYLOR, *Discovery of a pulsar in a binary system*, The Astrophysical Journal, 195 (1975), pp. L51–L53.

[24] P. KUMAR, T. CHU, H. FONG, H. P. PFEIFFER, M. BOYLE, D. A. HEMBERGER, L. E. KIDDER, M. A. SCHEEL, AND B. SZILAGYI, *Accuracy of binary black hole waveform models for aligned-spin binaries*, Physical Review D, 93 (2016), p. 104050.

[25] A. LE TIEC AND J. NOVAK, *Theory of gravitational waves*, (2016).

[26] C. MESSICK, K. BLACKBURN, P. BRADY, P. BROCKILL, K. CANNON, R. CARIOU, S. CAUDILL, S. J. CHAMBERLIN, J. D. E. CREIGHTON, R. EVERETT, C. HANNA, D. KEPPEL, R. N. LANG, T. G. F. LI, D. MEACHER, A. NIELSEN, C. PANKOW, S. PRIVITERA, H. QI, S. SACHDEV, L. SADEGHIAN, L. SINGER, E. G. THOMAS, L. WADE,

M. WADE, A. WEINSTEIN, AND K. WIESNER, *Analysis framework for the prompt discovery of compact binary mergers in gravitational-wave data*, Phys. Rev. D, 95 (2017), p. 042001.

[27] B. D. METZGER AND E. BERGER, *What is the Most Promising Electromagnetic Counterpart of a Neutron Star Binary Merger?*, , 746 (2012), p. 48.

[28] B. D. METZGER AND E. BERGER, *What is the most promising electromagnetic counterpart of a neutron star binary merger?*, The Astrophysical Journal, 746 (2012), p. 48.

[29] C. W. MISNER, K. S. THORNE, J. A. WHEELER, AND W. GRAVITATION, *Freeman and company*, San Francisco, (1973), p. 891.

[30] S. NISSANKE, M. KASLIWAL, AND A. GEORGIEVA, *Identifying elusive electromagnetic counterparts to gravitational wave mergers: an end-to-end simulation*, The Astrophysical Journal, 767 (2013), p. 124.

[31] A. H. NITZ, T. DAL CANTON, D. DAVIS, AND S. REYES, *Rapid detection of gravitational waves from compact binary mergers with pycbc live*, Phys. Rev. D, 98 (2018), p. 024050.

[32] OWEN AND SATHYAPRAKASH, *Matched filtering of gravitational waves from inspiraling compact binaries: Computational cost and template placement*, Physical Review D, 60 (1999), p. 022002.

[33] B. J. OWEN, *Search templates for gravitational waves from inspiraling binaries: Choice of template spacing*, Phys. Rev. D, 53 (1996), pp. 6749–6761.

[34] B. J. OWEN AND B. S. SATHYAPRAKASH, *Matched filtering of gravitational waves from inspiraling compact binaries: Computational cost and template placement*, 1998.

[35] J. RANA, A. SINGHAL, B. GADRE, V. BHALERAO, AND S. BOSE, *An optimal method for scheduling observations of large sky error regions for finding optical counterparts to transients*, 2016.

[36] B. SCHUTZ, *A First Course in General Relativity*, Cambridge University Press, 2009.

[37] L. P. SINGER, H.-Y. CHEN, D. E. HOLZ, W. M. FARR, L. R. PRICE, V. RAYMOND, S. B. CENKO, N. GEHRELS, J. CANNIZZO, M. M. KASLIWAL, ET AL., *Going the distance: mapping host galaxies of ligo and virgo sources in three dimensions using local cosmography and targeted follow-up*, The Astrophysical Journal Letters, 829 (2016), p. L15.

[38] L. P. SINGER AND L. R. PRICE, *Rapid bayesian position reconstruction for gravitational-wave transients*, Physical Review D, 93 (2016), p. 024013.

[39] V. SRIVASTAVA, K. R. NAYAK, AND S. BOSE, *Toward low-latency coincident precessing and coherent aligned-spin gravitational-wave searches of compact binary coalescences with particle swarm optimization*, 2018.

[40] S. A. USMAN ET AL., *The PyCBC search for gravitational waves from compact binary coalescence*, Class. Quant. Grav., 33 (2016), p. 215004.

[41] S. A. USMAN, A. H. NITZ, I. W. HARRY, C. M. BIWER, D. A. BROWN, M. CABERO, C. D. CAPANO, T. DAL CANTON, T. DENT, S. FAIRHURST, ET AL., *The pycbc search for gravitational waves from compact binary coalescence*, Classical and Quantum Gravity, 33 (2016), p. 215004.

[42] J. VEITCH, V. RAYMOND, B. FARR, W. FARR, P. GRAFF, S. VITALE, B. AYLOTT, K. BLACKBURN, N. CHRISTENSEN, M. COUGHLIN, ET AL., *Parameter estimation for compact binaries with ground-based gravitational-wave observations using the lalinference software library*, Physical Review D, 91 (2015), p. 042003.

[43] Y. WANG AND S. D. MOHANTY, *Particle swarm optimization and gravitational wave data analysis: Performance on a binary inspiral testbed*, Physical Review D, 81 (2010), p. 063002.

[44] J. WEBER, *Detection and generation of gravitational waves*, Physical Review, 117 (1960), p. 306.

[45] J. M. WEISBERG AND J. H. TAYLOR, *Relativistic binary pulsar b1913+ 16: Thirty years of observations and analysis*, arXiv preprint astro-ph/0407149, (2004).